 DOI: 10.17344/acsi.2016.3109 *Acta Chim. Slov.* **2017,** *64,* 202–207

Scientific paper

Mn(II), Zn(II) and Cd(II) Complexes Based on Oxadiazole Backbone Containing Carboxyl Ligand: Synthesis, Crystal Structure, and Photoluminescent Study

Li-Na Wang, Lin Fu, Jia-Wei Zhu, Yu Xu, Meng Zhang, Qi You, Peng Wang and Jie Qin*

School of Life Sciences, Shandong University of Technology, Zibo 255049, P. R. China

** Corresponding author: E-mail: qinjietutu@163.com*
Tel.: 0086-533-2780271; Fax: 0086-533-2781329

Received: 26-11-2016

Abstract

Three coordination polymers, $[Cd(L)_2(H_2O)_2]_n$ (**1**), $[Zn(L)_2(H_2O)_2]_n$ (**2**) and $[Mn(L)_2]_n$ (**3**) were prepared by reacting 5-(3-pyridyl)-1,3,4-oxadiazole-2-thioacetic acid (**HL**) with corresponding metal acetate in DMF/CH_3CN medium under solvothermal condition. The isolated complexes were characterized by elemental analysis and infrared spectroscopy. The X-ray crystallographic analysis revealed double strand structure of **1** and **2**, and 3D framework of **3**. The different structures of these complexes indicate that the configuration of the ligand and the reaction condition play a key role in self-assemble of complexes **1**–**3**. Furthermore, photoluminescent properties of **1** and **2** were also studied in the solid state.

Keywords: Oxadiazole ligand; solvent thermal synthesis; crystal structure; photoluminescent property

1. Introduction

Nowadays, more and more attention has been paid to coordination compounds with various of topological structures and potential promising applications ranging from functional material to therapeutic agent.[1–6] Many factors need to be considered during the self-assembly process of coordination compound, including the nature of the metal ion, the well-designed organic ligand, the auxiliary ligand, the solvent medium, the pH value, the temperature, and so on.[7] Therefore the rational design and precise crystal engineering of coordination compounds with desired structures and specific properties still remain a challenge.[8] According to previously reported work, the choice of organic ligand has been verified as a decisive role in the construction of the overall architectures of coordination polymers, as the organic spacer serves to link metal nodes and to propagate the structural information.[9,10]

Rigid linear organic ligands such as 4,4'-bipyridine and its derivatives are well adopted in generating polymers bearing linear chain,[11] honeycomb-like,[12] square-like,[13] or brick-wall-like structures.[14,15] While the bent organic ligands can offer the possibility of constructing novel polymer network owing to their variable conformation.[15] 1,3,4-Oxadiazole is an intensively investigated class of bent organic bridging moiety due to its convenient synthesis as well as the versatile coordination mode.[9,16–18] Coordination polymers, with structures like helical chain,[19] zeolite-like net,[16] and 3-fold interpenetrated 3D framework,[15] have been reported by Dong group. They are based on symmetric 2,5-diaryl-1,3,4-oxadiazole containing pyridyl, aminophenyl or cyanophenyl groups as terminal coordination sites. Herein we focus on the coordination behavior of 5-(3-pyridyl)-1,3,4-oxadiazole-2-thioacetate (**L**), which is mostly based upon the following considerations. (i) **L** is an unsymmetric ligand bearing both pyridine and carboxyl groups bridged by the oxadiazole backbone. Hence **L** can show diverse coordination modes. Especially the carboxyl group can feature unidentate, chelate or bridging fashions.[20] (ii) **L** is a bent ligand, which can adopt either *gauche*- or *anti*-configuration in the self-assembly reaction (Scheme 1).[8,20] (iii) Heteroatoms such as N, O, and S of **L** could be considered as potential hydrogen bond acceptors to expand polymeric frameworks via hydrogen bonding interactions.[16] Coordination polymers based on **L** and its isomer 5-(4-pyridyl)-1,3,4-oxadiazole-2-thioacetate (**4-pyoa**) were first reported by Du et al. under the layer separation diffusion condition.[20]

Reaction of **HL** and **4-pyoa** with metal salts afforded 1D coordination polymers of $\{[M_2(4\text{-pyoa})_4(H_2O)_2](H_2O)_2\}_n$ (M = Co, Zn), anatase type network of $\{[Pb(4\text{-pyoa})_2](H_2O)\}_n$, 2D layer of $\{[Cu(L)_2(H_2O)](H_2O)_2\}_n$, and 3,6-connected 3D net of $[Cd(L)_2]_n$.[20] Indeed, this demonstrates that **HL** is well-tailored in constructing new polymers with attractive properties.

The aim of the presented work is the construction of complexes derived from **HL** under solvent thermal condition. The reactions of **HL** and $M(CH_3COO)_2$ (M = Cd, Zn, and Mn) in DMF/CH_3CN at 110 °C afford three polymers, $[Cd(L)_2(H_2O)_2]_n$ (**1**), $[Zn(L)_2(H_2O)_2]_n$ (**2**) and $[Mn(L)_2]_n$ (**3**). Herein, the preparation, and crystallographic analyses of these complexes are described. Moreover, luminescent properties of **1** and **2** were investigated in the solid state.

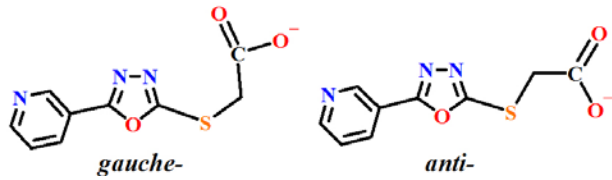

Scheme 1. Two possible configurations of **L**.

2. Experimental

2. 1. Physical Measurements and Materials

Reagents and solvents were purchased commercially from Aladdin Industrial Corporation (China) and used without further purification. The starting compound **HL** was synthesized according to the literature method.[20,21] The IR spectra were taken on a Vector22 Bruker spectrophotometer (400–4000 cm^{-1}) prepared as KBr pellets. Elemental analyses were performed on a Perkin-Elmer model 2400 analyzer. Fluorescence spectra were recorded on Cary Eclipse spectrofluorimeter (Varian, Australia) at room temperature.

2. 2. General Procedure for the Synthesis of Complexes 1–3

HL (0.1 mmol) and metal acetate salts (0.2 mmol) in 10 mL mixed solvent of DMF/CH_3CN (v/v = 1:1) were sealed in a 25 mL Teflon cup. The mixture was heated at 110 °C for 3 days and cooled to room temperature at a rate of 5°C/h. Yellow crystals were obtained.

$[Cd(L)_2(H_2O)_2]_n$ (**1**) Yield: 15.8 mg (51% on the basis of **HL**). The IR (KBr, cm^{-1}): 3446, 3098, 3033, 1607, 1577, 1474, 1462, 1438, 1393, 1222, 1198, 1091, 1049, 1031, 999, 960, 821, 715, 701, 684, 640, 443. Anal. Calcd. for $C_{18}H_{16}CdN_6O_8S_2$: C, 34.82; H, 2.60; N, 13.53. Found: C, 34.92; H, 2.59; N, 13.57%.

$[Zn(L)_2(H_2O)_2]_n$ (**2**) Yield: 13.8 mg (48% on the basis of **HL**). IR (KBr, cm^{-1}): 3468, 3085, 3067, 2985, 1646, 1614, 1459, 1417, 1364, 1326, 1191, 1087, 1052, 1004, 959, 820, 712, 698, 650, 537. Anal. Calcd. for $C_{18}H_{16}ZnN_6O_8S_2$: C, 37.67; H, 2.81; N, 14.64. Found: C, 37.82; H, 2.80; N, 14.69%.

$[Mn(L)_2]_n$ (**3**) Yield: 8.4 mg (32% on the basis of **HL**). IR (KBr, cm^{-1}): 3033, 1574, 1462, 1393, 1196, 1088, 1046, 996, 921, 819, 679, 639, 441. Anal. Calcd. for $C_{18}H_{12}MnN_6O_6S_2$: C, 40.99; H, 2.93; N:15.93. Found: C, 41.12; H, 2.91; N, 15.99%.

Table 1. Crystallographic data for **1–3**.

	1	**2**	**3**
Empirical formula	$C_{18}H_{16}CdN_6O_8S_2$	$C_{18}H_{16}ZnN_6O_8S_2$	$C_{18}H_{12}MnN_6O_6S_2$
M_r	620.89	573.86	527.40
Crystal System	triclinic	triclinic	monoclinic
Space group	P–1	P–1	C2/c
a (Å)	7.4145(11)	7.3585(6)	25.302(3)
b (Å)	7.6738(11)	7.4216(7)	10.6816(11)
c (Å)	10.6697(15)	10.7069(9)	7.1462(7)
α (°)	88.064(4)	88.979(3)	90.00
β (°)	82.611(4)	82.757(2)	95.747(3)
γ (°)	74.497(4)	73.709(3)	90.00
V (Å^3)	580.13(14)	556.67(8)	1921.7(3)
Z	1	1	4
ρ_c (g cm^{-3})	1.777	1.712	1.823
F(000)	310	292	1068
T / K	298(2)	298(2)	298(2)
μ(Mo-Kα)/ mm^{-1}	1.179	1.351	0.960
GOF (F^2)	1.131	1.084	1.107
Data / restraints / parameters	2614 / 0 / 160	2531 / 0 / 160	2207 / 0 / 150
R_1[a], wR_2[b] ($I>2\sigma(I)$)	0.0205, 0.0540	0.0245, 0.0611	0.0248, 0.0662

[a] $R_1 = \Sigma||Fo| - |Fc||/\Sigma|Fo|$. [b] $wR_2 = [\Sigma w(Fo^2 - Fc^2)^2/\Sigma w(Fo^2)]^{1/2}$

2. 3 Determination of Crystal Structures

X-ray intensity data for crystals **1–3** were collected on a Bruker SMART APEX CCD-based diffractometer (Mo Kα radiation, λ = 0.71073 Å) at 298 K. The raw frame data were integrated into SHELX format reflection files and corrected for Lorentz and polarization effects using SAINT.[22] Multi-scan absorption corrections were applied by SADABS.[23] All the structures were solved by direct methods and refined by full-matrix least-square methods applying SHELXL program package.[24] Anisotropic thermal parameters were used to refine all non-hydrogen atoms. H atoms of C–H were geometrically generated and refined with isotropic thermal parameters riding on the parent atoms. The H atoms of water molecules were fixed by difference Fourier maps with O–H = 0.85(2) Å, H···H = 1.44(2) Å and U_{iso}(H) = 1.5U_{eq}(O). Details of crystallographic parameters, data collection, and refinements are summarized in Table 1. Relevant bond distances and bond angles are given in Tables 2, 3 and S1.

3. Results and Discussion

3. 1. Synthesis and General Characterization

The mixing of metal salts and carboxylic ligand solution resulted in precipitation in traditional aqueous reaction system therefore solvothermal synthesis was adopted. By performing parallel experiments, it was found that using $M(NO_3)_2$ or $M(ClO_4)_2$ (M = Cd, Zn, Mn) as the source of metal salts could also isolate these complexes, which indicates that the complexes are independent of the counter-anions of the metal salts. The acetate salts were found to achieve products in a somewhat higher crystal quality and yield.

3. 2. IR Spectra

The IR spectra of complexes **1–3** (see Figure S1, Supporting Information) exhibiting the absence of characteristic absorption bands of the carboxyl group (1718 cm^{-1} in **HL**) reveals the complete deprotonation. As a consequence, the antisymmetric ($\nu_{as}(COO^-)$) and symmetric ($\nu_s(COO^-)$) stretching vibrations of carboxylate groups appear. The separation value $\Delta\nu$ between $\nu_{as}(COO^-)$ and $\nu_s(COO^-)$ can be used to identify the coordination mode of the carboxylate ligand.[25,26] The $\Delta\nu$ value is 214 cm^{-1} for **1**, 229 cm^{-1} for **2**, indicating a monodentate coordination mode of carboxylate group. While the $\Delta\nu$ value for **3** is 181 cm^{-1} indicative of bidentate carboxylate coordination. These IR results are in agreement with the crystal structural analyses.

3. 3. Crystal Structures

X-ray single-crystal diffraction reveals that complexes **1** and **2** are isostructural and crystallize in the same triclinic $P\bar{1}$ space group with similar cell parameters. Therefore only the structure of **1** is described here in detail as a representative example. The ORTEP plots of complexes **1** and **2** with atomic numbering scheme are shown in Figures 1 and S2

As drawn in Figure 1, the Cd^{II} ion is located at the inversion center, and the asymmetric unit of compound **1** is composed of one Cd^{II} ion with the occupancy of 0.5, one L^{1-} ligand, and one coordinated water molecule. The central Cd^{II} is six coordinate with two N and two O atoms from four crystallographically independent L^{1-}, and two water O atoms. The coordination geometry of the $\{CdN_2O_4\}$ can be described as an almost perfect octahe-

Table 2. Selected bond distances (Å) and angles (°) for complex **1**.

Cd1–O4	2.3030(13)	Cd1–O3^{iii}	2.2584(14)
Cd1–N1	2.3703(14)	S1–C7	1.7275(18)
S1–C8	1.8042(19)	O2–C9	1.242(2)
O3–C9	1.251(2)		
N1–Cd1–N1^{i}	180.000(1)	O3^{iii}–Cd1–N1	90.24(6)
O4^{i}–Cd1–N1^{i}	91.59(5)	O3^{iii}–Cd1–O4	91.31(5)
O3^{ii}–Cd1–O4	88.69(5)	O4–Cd1–O4^{i}	180.0
O3^{ii}–Cd1–N1	89.76(6)	O4^{i}–Cd1–N1	88.41(5)
C7–S1–C8	98.83(9)		

Symmetry codes: (i) –*x*, –*y* + 1, –*z* + 2; (ii) –*x* + 1, –*y* + 1, –*z* + 1; (iii) *x* – 1, *y*, *z* + 1

Table 3. Selected bond distances (Å) and angles (°) for complex **3**

Mn1–O2	2.1024(10)	Mn1–O3^{ii}	2.1878(10)
Mn1–N1^{iii}	2.3479(11)	S1–C7	1.7235(14)
S1–C8	1.7969(14)	O2–C9	1.2453(17)
O3–C9	1.2485(17)		
N1^{iii}–Mn1–N1^{i}	94.98(6)	O2–Mn1–O2^{iv}	93.00(6)
O2–Mn1–O3^{v}	103.46(4)	O2^{i}–Mn1–O3^{v}	92.20(4)
O3$^{\#v}$–Mn1–O3$^{\#ii}$	157.28(6)	O2–Mn1–N1^{iii}	176.41(4)
O2^{iv}–Mn1–N1^{iii}	86.11(4)	O3^{v}–Mn1–N1^{iii}	80.06(4)
O3^{ii}–Mn1–N1^{iii}	84.63(4)	C7–S1–C8	98.76(6)

Symmetry codes: (i) –*x* + 3/2, *y* – ½, –*z* + ½; (ii) *x*, –*y* + 1, *z* – ½; (iii) *x* – ½, *y* – ½, *z*; (iv) –*x* + 1, *y*, –*z* + ½; (v) –*x* + 1, –*y* + 1, –*z* + 1

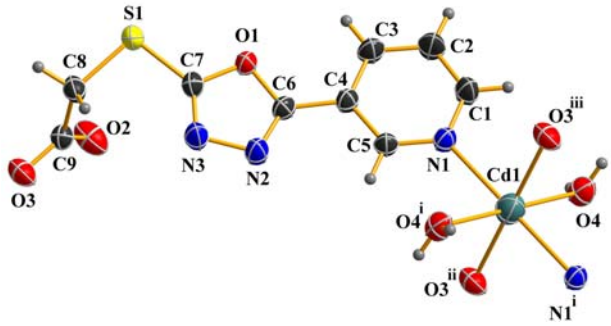

Figure 1. Coordination environment of Cd^{II} in **1**. Symmetry codes: (i) –*x*, –*y* + 1, –*z* + 2; (ii) –*x* + 1, –*y* + 1, –*z* + 1; (iii) *x* – 1, *y*, *z* + 1.

dron, which is reflected by the axial N1–Cd–N1^{i} 180.0°, and the sum of the equatorial bond angels being 360.0°. The *gauche* style of the ligand is observed in complex **1**, which was confirmed by the value of the torsion angle of C7–S1–C8–C9 being –70.94(15)°.

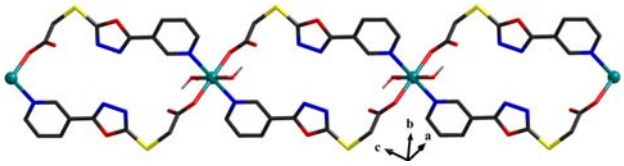

Figure 2. 1D coordination framework of **1**.

Du and coworkers have prepared the complex $[Cd(L)_2]_n$ (**1A**) in CH_3OH/H_2O-NaOH mixed solvent system at room temperature using $Cd(NO_3)_2$ and **HL**.[20] In **1A**, the octahedral coordination sphere of Cd^{II} is provided by four carboxylate O and two pyridyl N atoms coming from six separated ligands. The authors ascribed this coordination geometry to the metal–ligand synergistic effect that the Cd^{II} ion with larger radii is capable of holding six ligands around it. In **1A**, the ligand serves as a 3-connected node resulting in the 3D rutile framework. While in complex **1**, the pyridyl and the carboxylic groups both adopted the monodentate coordination mode acting as 2-connected node. The Cd^{II} ions are bridged by paired **L** ligands. As a consequence, 1-D double-strand coordination array of **1** is formed running along [1 0 –1] direction with Cd···Cd separation of 12.1848(14) Å (Figure 2). The Cd–$N_{pyridyl}$ bond length (2.3703(14) Å) is comparable to that in **1A** (2.373(2) Å), while the Cd–$O_{carboxylic}$ bond length in **1** being 2.2584(14) Å is longer than that in **1A** 2.291(2) Å. The intra-chain hydrogen bond interactions were found between the uncoordinated carboxylic O atoms and the coordinated water molecules (O4–H4B···O2^{iii}, symmetric code: (iii) $x - 1, y, z + 1$).

Analysis of the crystal packing of **1** reveals the existence of two types of inter-chain hydrogen bonds, including O4–H4A···O2^{iv} and O4–H4A···S1^{iv} (symmetric code: (iv): $-x, -y + 1, z + 1$) between the water ligands and the uncoordinated carboxylic O atoms as well as S atoms. Therefore, these 1D chains are connected through these hydrogen bonds, forming a two-dimensional supramolecular layer along the [001] plane, as depicted in Figure 3.

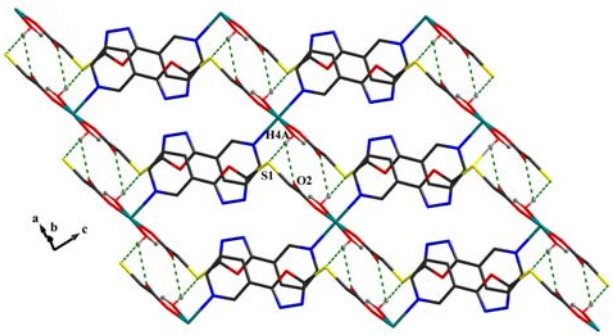

Figure 3. View of the 2D hydrogen-bonding supramolecular layer in **1**.

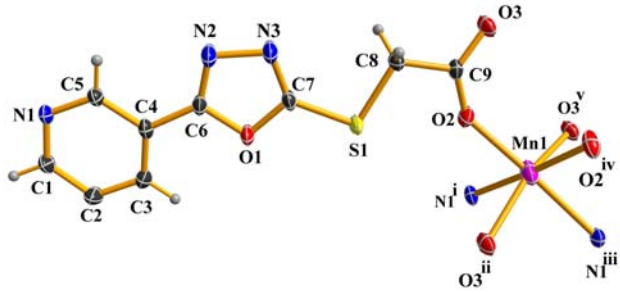

Figure 4. The coordination environment of Mn(II) in **3** at 50% probability displacement. Symmetry codes: (i) $-x + 3/2, y - ½, -z + ½$; (ii) $x, -y + 1, z - ½$; (iii) $x - ½, y - ½, z$; (iv) $-x + 1, y, -z + ½$; (v) $-x + 1, -y + 1, -z + 1$.

Polymer **3** crystallized in monoclinic *C*2/*c* space group. As illustrated in Figure. 4, the independent unit of **3** is composed of half Mn(II) cation and one deprotonated ligand L^{1-}. The L^{1-} serves as a μ_3-bridging ligand in **3**, which is identical to that in complex **1A.** The Mn center is hexa-coordinated in distorted octahedron coordination geometry and is bonded by four carboxyl oxygen atoms from four L^{1-} anions [Mn1–O2 = 2.1024(10) Å; Mn1–O3 = 2.1878(10) Å], and two pyridine nitrogen atoms from the other two ligands with Mn–N bond lengths of 2.3479(11) Å. The N1^{i}, O3^{ii}, O2^{iv} and O3^{v} are located in the equatorial plane, while the O2 and N1^{iii} atoms occupy the axial positions. The difference of coordination geometry between Mn^{II} in **3** and Cd^{II} in **1A** lies in that the pyridine N atoms are in the axial positions in **1A**.[20] The Mn–O and Mn–N bond distances are close to other manganese complexes derived from (4-pyridylthio)acetic acid (PTA), such as [(Mn-salen)PTA] and $[Mn(PTA)_2(H_2O)]_n$.[27,28] Compared with complexes **1** and **2**, the ligand adopted *anti*-configuration in **3** as evidenced by the torsion angle of C7–S1–C8–C9 being –167.9°.

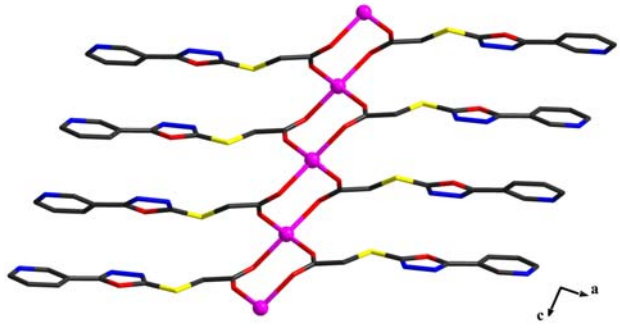

Figure 5. The1D chain structure in **3**.

In **3** the adjacent Mn^{II} centers are doubly bridged by the carboxyl groups of L^{1-}, forming an infinite chain structure along the *c* direction, with a Mn···Mn distance of 4.567(4) Å (Figure 5). In each L^{1-} ligand, the mean plane of the carboxylate group and the plane of the pyridine group are inclined to each other with a dihedral angle of 19.2°. Such 1D chains are aligned side by side in the *ab* plane, and are further linked together by Mn1–N1 linkages, eventually forming the three dimensional network of **3** (Figure 6).

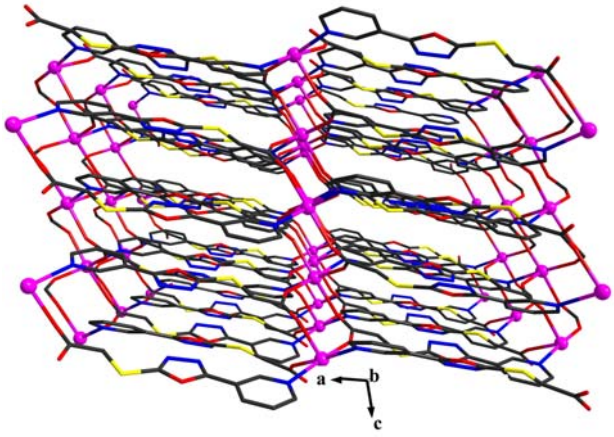

Figure 6. The 3D network of **3**.

3. 4. Photoluminescent Properties

Taking into account that coordination compounds based on d^{10} metal centers are promising candidates for photoactive materials with potential applications,[29,30] the ambient temperature photoluminescent properties of **1** and **2** as well as the free ligand **HL** were measured in the solid state.

As depicted in Figure 7, upon excitation at 290 nm, the free compound **HL** has an emission band maxima at 325 nm. The emission of **HL** can be assigned to the π* to π and π* to n intraligand transitions.[31,32] As Cd^{2+} or Zn^{2+} ions are difficult to oxidize or reduce owning to their d^{10} configuration,[33] the emission spectra of complexes **1** and **2** are similar with that of **HL**. Hence the luminescent emissions of **1** and **2** are attributed to the intraligand transition. Moreover, approximately a three-time increase in the luminescence intensity was observed for complexes compared with the free ligand. The red shifts (10 nm for **1** and 17 nm for **2**) and enhancement of luminescence intensity of the complexes may be ascribed to the deprotonation and coordination to metal ions, which can effectively enhance the rigidity of **HL** and further reduce the loss of energy by radiationless decay of the intraligand emission excited state.[34]

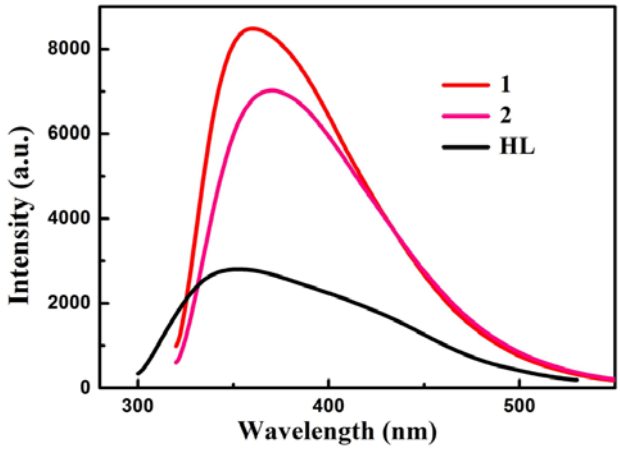

Figure 7. Solid state emission spectra of compounds **HL**, **1** and **2** at room temperature.

4. Conclusions

To sum up, three Cd(II), Zn(II) and Mn(II) coordination polymers based on semirigid asymmetric ligand 5-(3-pyridyl)-1,3,4-oxadiazole-2-thioacetate were successfully prepared. Complexes **1** and **2** are double-strand structures, and two-dimensional supramolecular networks were further observed through O–H···O and O–H···S hydrogen bonding interactions. While **3** features three-dimensional framework. The structural diversity reveals that the configuration of the ligand and the reaction condition play an important role during the self-assembly process of complexes **1**–**3**. In addition, complexes **1** and **2** exhibit intense blue fluorescent emission indicating promising candidates for functional inorganic-organic photoactive materials.

5. Supplementary Material

Crystallographic data (excluding structure factors) for the structural analysis have been deposited with the Cambridge Crystallographic Data Center as supplementary publication Nos. CCDC 1518672 (**1**), 1518673 (**2**), and 1518674 (**3**). Copies of the data can be obtained free of charge *via* www.ccdc.ac.uk/conts/retrieving.html (or from The Director, CCDC, 12 Union Road, Cambridge CB2 1EZ, UK, Fax: +44-1223-336-033. E-mail: deposit@ccdc.cam.ac.uk).

6. Acknowledgment

This work was supported by the National College Students' Innovative and Entrepreneurial Training Plan of China (201510433068) and Natural Science Foundation of Shandong Province (ZR2011HM065).

7. References

1. W. J. Gee, L. K. Cadman, H. A. Hamzah, M. F. Mahon, P. R. Raithby, A. D. Burrows, *Inorg. Chem.* **2016**, *55*, 10839–

10842. https://doi.org/10.1021/acs.inorgchem.6b01917
2. J. Qin, N. Qin, C. H. Geng, J. P. Ma, Q. K. Liu, D. Wu, C. W. Zhao, Y. B. Dong, *CrystEngComm.* **2012**, *14*, 8499–8508. https://doi.org/10.1039/c2ce25561h
3. R. Vafazadeh, A. C. Willis, *Acta Chim. Slov.* **2016**, *63*, 186–192. https://doi.org/10.17344/acsi.2016.2263
4. J. Qin, S. S. Zhao, Y. P. Liu, Z. W. Man, P. Wang, L. N. Wang, Y. Xu, H. L. Zhu, *Bioorg. Med. Chem. Lett.* **2016**, *26*, 4925–4929. https://doi.org/10.1016/j.bmcl.2016.09.015
5. J. Qin, Q. Yin, S. S. Zhao, J. Z. Wang, S. S. Qian, *Acta Chim. Slov.* **2016**, *63*, 55–61. https://doi.org/10.17344/acsi.2015.1918
6. J. X. Qi, S. C. Liang, Y. Gou, Z. L. Zhang, Z. P. Zhou, F. Yang, H. Liang, *Eur. J. Med. Chem.* **2015**, *96*, 360–368. https://doi.org/10.1016/j.ejmech.2015.04.031
7. S. Mohapatra, S. Adhikari, H. Riju, T. K. Maji, *Inorg. Chem.* **2012**, *51*, 4891–4893. https://doi.org/10.1021/ic300237e
8. M. Du, X. J. Zhao, Y. Wang, *Dalton Trans.* **2004**, 2065–2072. https://doi.org/10.1039/B403498H
9. Y. B. Dong, J. P. Ma, M. D. Smith, R. Q. Huang, B. Tang, D. S. Guo, J. S. Wang, H. C. zur Loye, *Solid State Sci.* **2003**, *5*, 601–610. https://doi.org/10.1016/S1293-2558(03)00041-4
10. Y. Bai, J. L. Wang, D. B. Dang, M. M. Li, J. Y. Niu, *CrystEngComm.* **2012**, *14*, 1575–1581. https://doi.org/10.1039/C1CE06030A
11. A. J. Blake, N. R. Champness, P. Hubberstey, W. S. Li, M. A. Withersby, M. Schröder, *Coord. Chem. Rev.* **1999**, *183*, 117–138. https://doi.org/10.1016/S0010-8545(98)00173-8
12. L. R. MacGillivray, S. Subramamian, M. J. Zaworotko, *J. Chem. Soc., Chem. Commun.* **1994**, 1325–1326. https://doi.org/10.1039/c39940001325
13. M. Fujita, Y. J. Kwon, S. Washizu, K. Ogura, *J. Am. Chem. Soc.* **1994**, *116*, 1151–1152. https://doi.org/10.1021/ja00082a055
14. M. Fujita, Y. J. Kwon, O. Sasaki, K. Yamaguchi, K. Ogura, *J. Am. Chem. Soc.* **1995**, *117*, 7287–7288. https://doi.org/10.1021/ja00132a046
15. Y. B. Dong, H. X. Xu, J. P. Ma, R. Q. Huang, *Inorg. Chem.* **2006**, *45*, 3325–3343. https://doi.org/10.1021/ic052158w
16. Y. B. Dong, J. Y. Chen, R. Q. Huang, *Inorg. Chem.* **2003**, *42*, 5699–5706. https://doi.org/10.1021/ic034306t
17. W. Zhang, W. He, X. R. Guo, Y. W. Chen, L. M. Wu, D. C. Guo, *J. Alloy Compd.* **2015**, *620*, 383–389. https://doi.org/10.1016/j.jallcom.2014.09.153
18. C. Köhler, E. Rentschler, *Eur. J. Inorg. Chem.* **2016**, 1955–1960. https://doi.org/10.1002/ejic.201501278
19. J. P. Ma, Y. B. Dong, R. Q. Huang, M. D. Smith, C. Y. Su, *Inorg. Chem.* **2005**, *44*, 6143–6145. https://doi.org/10.1021/ic0505504
20. Z. H. Zhang, M. Du, *CrystEngComm.* **2008**, *10*, 1350–1357. https://doi.org/10.1039/b803736a
21. R. H. Omar, B. A. El-Fattah, *Egypt. J. Pharm. Sci.* **1985**, *24*, 49–56.
22. Bruker, SMART and SAINT. Bruker AXS Inc., Madison, Wisconsin, USA, **2002**.
23. G. M. Sheldrick, SADABS. Program for Empirical Absorption Correction of Area Detector, University of Göttingen, Germany, **1996**.
24. G. M. Sheldrick, *Acta Crystallogr.* **2008**, *A64*, 112–122. https://doi.org/10.1107/S0108767307043930
25. X. H. Bu, M. L. Tong, Y. B. Xie, J. R. Li, H. C. Chang, S. Kitagawa, J. Ribas, *Inorg. Chem.* **2005**, *44*, 9837–9846. https://doi.org/10.1021/ic050886d
26. M. Almáši, Z. Vargová, D. Sabolová, J. Kudláčová, D. Hudecová, J. Kuchár, L.Očenášová, K. Györyová, *J. Coord. Chem.* **2015**, *68*, 4423–4443. https://doi.org/10.1080/00958972.2015.1101074
27. H. Byrd, R. S. Buff, J. M. Butler, G. M. Gray, *J. Chem. Crystallogr.* **2003**, *33*, 515–519. https://doi.org/10.1023/A:1024211021089
28. W. Chiang, D. M. Ho, D. V. Engen, M. E. Thompson, *Inorg. Chem.* **1993**, *32*, 2886–2893. https://doi.org/10.1021/ic00065a015
29. L. Y. Kong, X. H. Lu, Y. Q. Huang, H. Kawaguchi, Q. Chu, H. F. Zhu, W. Y. Sun, *J. Solid State Chem.* **2007**, *180*, 331–338. https://doi.org/10.1016/j.jssc.2006.10.029
30. Y. J. Cui, Y. F. Yue, G. D. Qian, B. L. Chen, *Chem. Rev.* **2012**, *112*, 1126–1162. https://doi.org/10.1021/cr200101d
31. Y. D. Zhang, Z. W. Du, X. G. Luo, *Z. Anorg. Allg. Chem.* **2015**, *641*, 2637–2640. https://doi.org/10.1002/zaac.201500617
32. L. Croitor, E. B. Coropceanu, A. V. Siminel, O. Kulikova, V. I. Zelentsov, T. Datsko, M. S. Fonari, *CrystEngComm.* **2012**, *14*, 3750–3758. https://doi.org/10.1039/c2ce00020b
33. A. Thirumurugan, S. Natarajan, *Dalton Trans.* **2004**, *28*, 2923–2928. https://doi.org/10.1039/b408403a
34. J. F. Fang, J. X. Cheng, S. T. Huang, J. Zhang, C. Q. Ni, Y. J. Xiong, Q. Chen, F. F. Zhu, Y. Li, S. T. Yue, *Z. Anorg. Allg. Chem.* **2015**, *641*, 2657–2663. https://doi.org/10.1002/zaac.201500613

Povzetek

Pripravili smo tri koordinacijske polimere $[Cd(L)_2(H_2O)_2]_n$ (**1**), $[Zn(L)_2(H_2O)_2]_n$ (**2**) in $[Mn(L)_2]_n$ (**3**) z reakcijo med 5-(3-piridil)-1,3,4-oksadiazol-2-tioocetno kislino (**HL**) z ustreznim kovinskim acetatom v mešanici DMF/CH_3CN pri solvotermalnih pogojih. Izolirane komplekse smo okarakterizirali z elementno analizo in infrardečo spektroskopijo. Rentgenska strukturna analiza razkrije strukturo dvojne vijačnice pri spojinah **1** in **2** ter 3D mrežo pri **3**. Različne strukture teh kompleksov kažejo, da imajo konfiguracija liganda in reakcijski pogoji ključno vlogo pri zlaganju v kristalno strukturo. Proučili smo tudi fotoluminiscenčne lastnosti **1** in **2** v trdnem stanju.